Diffraction tomography: perturbed vees in midpoint-offset space?

Marta Jo Woodward

ABSTRACT

In reflection seismic experiments, localized velocity anomalies cast shadows on underlying reflectors—creating anomalous time-shift patterns on expected arrival horizons in midpoint-offset space. When the velocity anomalies are larger than the dominant source wavelength of the experiment, these time-shift patterns may be predicted by ray-tracing and the time delays inverted for the velocity field using ray-theoretic, reflection tomography. When the velocity anomalies are on the order of the dominant source wavelength of the experiment, ray theory breaks down and wave effects must be incorporated in the inversion. The theory of diffraction tomography has been developed for this latter problem: it inverts the full, forward-scattered wavefield after linearization of the scalar wave equation through application of either the Born or Rytov approximations. SEP-51 contained an article proposing a simplified form of diffraction tomography, based on the perturbation of ray-theoretic time-shift patterns to account for diffraction effects instead of on full wavefield inversion. The results in that paper were promising but not perfect. This paper examines a slightly different method of modifying the ray-theoretic vee-patterns for wave phenomena than that described in SEP-51. The results are inferior to those of the previous paper; they fail to conclusively evaluate the potential of the approach.

INTRODUCTION

In reflection seismic experiments, localized velocity anomalies cast shadows on underlying reflectors—creating anomalous time-shift patterns on expected arrival horizons in midpoint-offset space. When the velocity anomalies are larger than the dominant source wavelength of the experiment, these time-shift patterns may be predicted by ray-tracing. The identification of the typically vee-shaped patterns is the basis of ray-theoretic, reflection tomography (Woodward, 1987).

When the velocity anomalies are on the order of the dominant source wavelength of the experiment, ray-theory breaks down and ray-tracing can no longer predict either the magnitude or the shape of the time-shift patterns. The theory of diffraction tomography has been developed for the inversion of such small-scale velocity anomalies, where wave effects and diffraction phenomena must be considered (Devaney, 1984; Slaney et al., 1984; Wu and Toksöz, 1987). The method relates the unknown velocity field to the wavefield measured at the receivers directly—without picking time shifts. The forward-scattered wavefield is inverted after linearization of the scalar wave equation through application of either the Born or Rytov approximations.

SEP-51 contained an article proposing a simplified form of diffraction tomography, based on the perturbation of ray-theoretic time-shift patterns to account for diffraction effects instead of on full wavefield inversion (Woodward, 1987). Working both from observations of vee-patterns produced by anomalies of the same scale as the dominant source wavelength, and from Huygens' principle, the paper suggested diffraction phenomena could be incorporated into ray-theoretic vee-patterns by smearing them in midpoint and damping them in offset. The basically empirical method yielded improved resolution of anomalies on the order of a half-wavelength, in comparison to ray-theoretic results.

This paper examines a slightly different method of modifying the ray-theoretic vee-patterns for wave phenomena than that proposed in SEP-51—corresponding to a different guess at how to forward model the diffraction effects of a small-scale velocity anomaly in a bandlimited experiment. The results are disappointing but interesting. They fail to conclusively determine the applicability of perturbed vees in midpoint-offset space to the problem of inverting reflection seismic data for small-scale velocity anomalies.

VEE-PATTERNS

The ray-theoretic and pseudo-wave-theoretic vee-patterns derived in SEP-51 are repeated in Figures 1a and 1b, respectively. A brief review of their construction follows; a more complete description of them and of the reflection seismic experiment for which they were designed may be found in the previous report. The patterns on the left correspond to the time-shift shadows cast in midpoint-offset space by a single anomaly located at the surface of a discretized, constant velocity background field; the patterns on the right correspond to the shadows cast by a single anomaly located half-way between the surface and the reflector. In both cases, the apex of the vee points to the position of the velocity anomaly on the midpoint axis. For the ray-theoretic vees, the intensity of the pattern at each midpoint-offset position is proportional to the path length travelled by the corresponding ray through the anomaly—and consequently to the time shift expected at that position. The wave-theoretic vees were derived from the ray-theoretic vees in two steps. First, to account

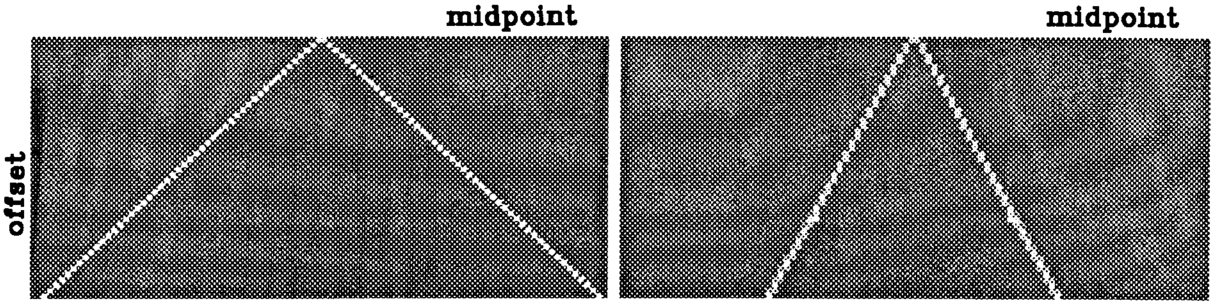

(a). Ray–theoretic vees

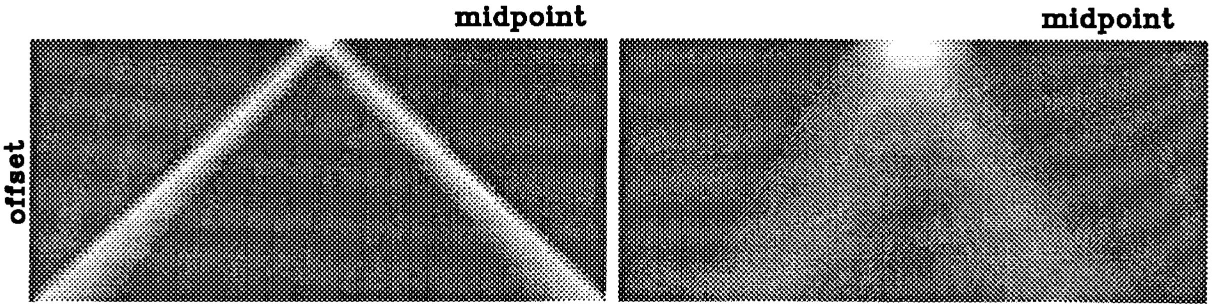

(b). Wave–theoretic vees of SEP–51

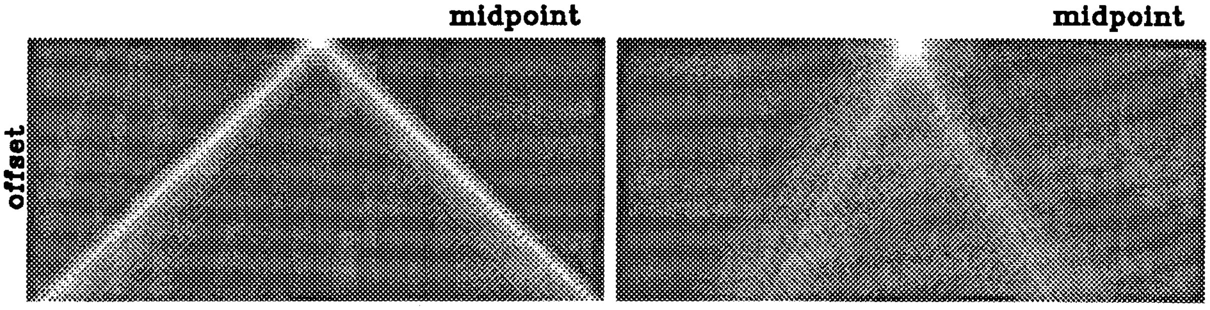

(c). Wave–theoretic vees of SEP–56

FIG. 1. Vee-patterns: the leftmost plots illustrate the time-shift shadow cast in midpoint-offset space by a single, square anomaly positioned at the surface; the rightmost plots illustrate the shadow for a similar anomaly positioned half-way between the surface and the reflector.

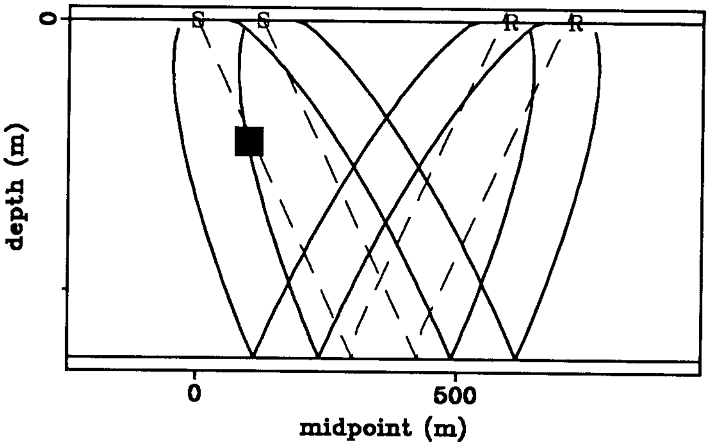

FIG. 2. Raypaths connecting source-receiver pairs for two neighboring midpoints are shown as dashed lines. The elliptical regions influencing the first half-wavelength of the corresponding band-limited source-receiver events are shown as heavy solid lines. Ray theory predicts detection of the square anomaly only at the midpoint on the left; wave theory predicts its detection at both midpoints.

for wavefront healing, the vees were damped in offset. The magnitudes along the ray-theoretic vees were multiplied by the square root of the ratio of the anomaly's cross-section to the Fresnel zone of the expanding source wave, as measured at their intersection. Second, the ray-theoretic vees were smeared in midpoint. For each offset on each vee, the dimensions of the elliptical region influencing the first half-wavelength of a source-receiver event in a homogeneous velocity field were calculated (Hagedoorn, 1954). The vees were then linearly tapered along midpoint from a ray-theoretic high point (defined by that midpoint where the source-receiver ray intersected the anomaly) out to a wave-theoretic low point (defined by that midpoint where the ellipse surrounding the source-receiver ray just grazed the anomaly). (See Figure 2 for the geometry of this argument.) From a forward modelling point of view, this procedure weights the midpoints by guessing the magnitudes of their time-shift responses to an anomaly positioned at the vee's apex.

The choice of a linear taper in midpoint was empirically determined in the previous paper. This paper examines a more thoughtful though less successful scheme for smearing the vees in midpoint. The effort to quantify the impact of an anomaly on the arrival time of each source-receiver event was accomplished in three steps. First, the ellipse bounding the region influencing the first half-wavelength of an event in a homogeneous velocity field was calculated for each midpoint-offset pair. Second, the raypaths determining the envelope of the ellipse were traced—in order to gauge the influence of the different regions of the ellipse on the arrival time of the corresponding source-receiver event. Third, a hit count was calculated from this ray-tracing for each square of the discretized background velocity field, and its square root was used to determine the weighting of the vees in midpoint. (The square root was taken in order to represent amplitude instead of energy, following Claerbout and Dellinger, 1986.) Figure 3 shows the geometry of this argument;

FIG. 3. The ellipse bounding the region influencing the first half-wavelength of a source-receiver event in a homogeneous velocity field and the raypaths determining its boundaries.

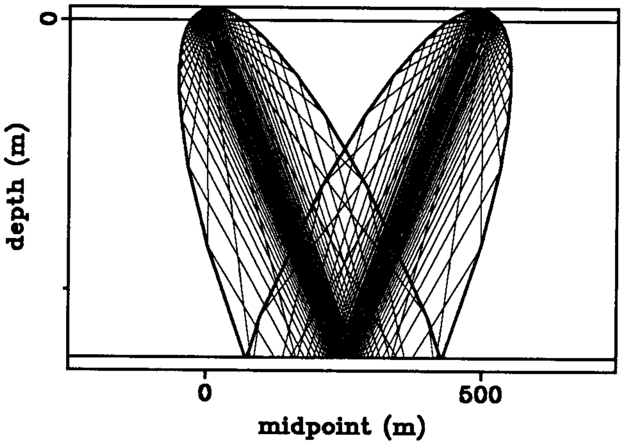

Figure 1c shows the resulting vee-patterns. The patterns drop off much more sharply in midpoint than the pseudo-wave-theoretic vees of the previous paper.

INVERSION RESULTS

The true velocity field and the results of inverting the bandlimited reflection data of SEP-51 with each of the three vee-patterns of Figure 1 are shown in Figure 4. The plots labelled (a), (b) and (c) are repeated from the previous paper; plot (d) is new. The first two inversions ran until they stopped converging, after 17 and 22 iterations and a 21% and 13% increase in the objective function, respectively. The third inversion was stopped after 15 iterations and a 16% increase in the objective function. (See the previous paper for a discussion of the objective function and optimization scheme.) Comparison of Figures 4c and 4d reveals that the new wave-theoretic vees did a surprisingly poor job of inverting the small-scale velocity anomalies. The method has placed artifacts at the edges of the anomalies, instead of locating the anomalies themselves. This result may be attributed to the steep drop-off in the vees with midpoint: the scheme compensates for the low weights on the outlying midpoints by overestimating the contributions of those vees adjacent to the true anomalies. Various efforts aimed at reducing the drop-off while retaining the basic quantitative argument were unsuccessful.

SUMMARY

At this point, the feasibility of inverting reflection seismic data for small-scale velocity anomalies by perturbing time-shift patterns in midpoint-offset space remains unclear. The method is based on the assumption that the time delays measured by crosscorrelating events influenced by a small anomaly may be linearly related

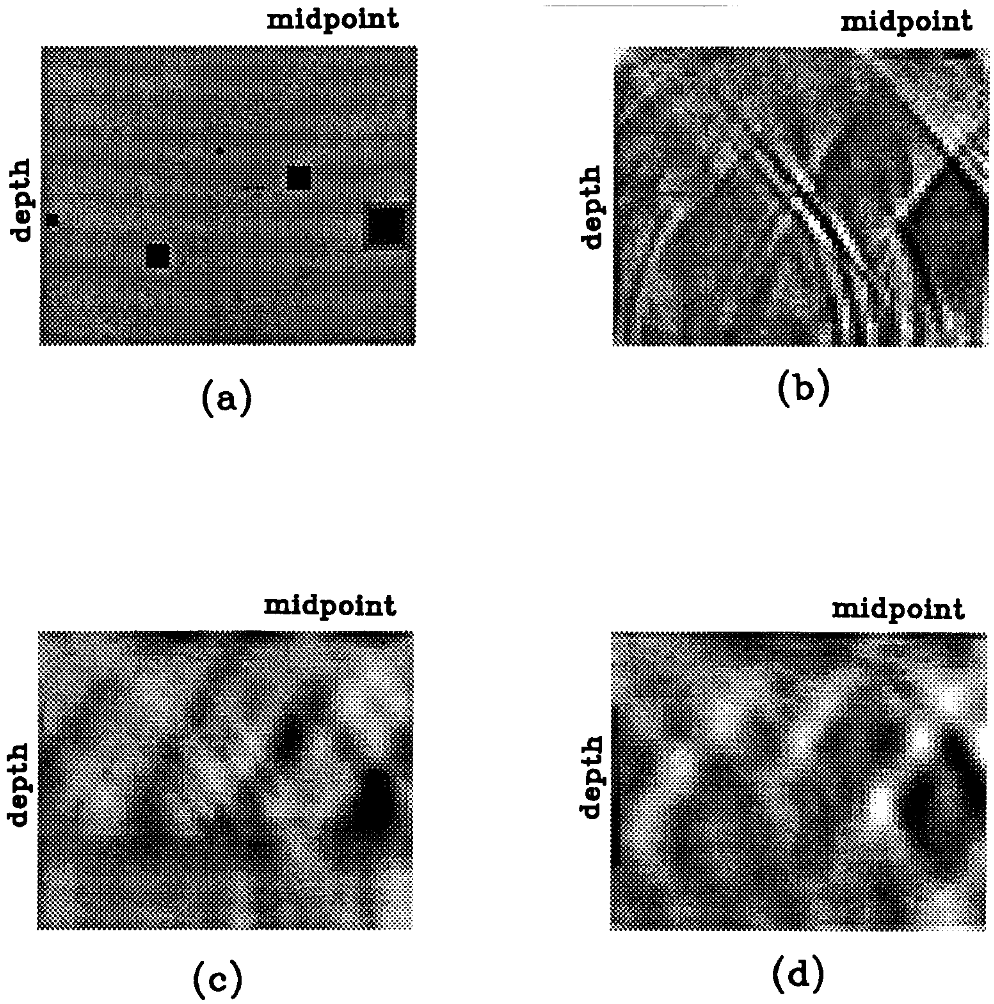

FIG. 4. Inversion results. (a). Velocity model. (b). Inversion with ray-theoretic vees. (c). Inversion with wave-theoretic vees of SEP-51. (d). Inversion with wave-theoretic vees of SEP-56.

(approximately) to the velocity field—that they do not represent indecipherable interference effects. Different schemes for quantitatively designing vee-patterns need to be devised. The method needs to be compared with full wavefield inversion diffraction tomography.

REFERENCES

Claerbout, J., and Dellinger, J., 1986, Eisner's reciprocity paradox and its resolution: SEP-50, pp. 99-102 and 107-112.

Devaney, A.J., 1984, Geophysical diffraction tomography: IEEE Transactions on Geoscience and Remote Sensing, vol. GE-22, no. 1, pp. 3-13.

Hagedoorn, J.G., 1954, A process of seismic reflection interpretation: Geophysical Prospecting, vol. 2, pp. 85-127.

Slaney, M., Kak, A.C., and Larsen, L.E., 1984, Limitations of imaging with first-order diffraction tomography: IEEE Transactions on Microwave Theory and Techniques, vol. MTT-32, no. 8, pp. 860-873.

Woodward, M.J., 1987, Reflection tomography: vees in midpoint-offset space: SEP-51, pp. 1-12.

Wu, R., and Toksöz, M.N., 1987, Diffraction tomography and multisource holography applied to seismic imaging: Geophysics, vol. 52, no. 1, pp. 11-25.

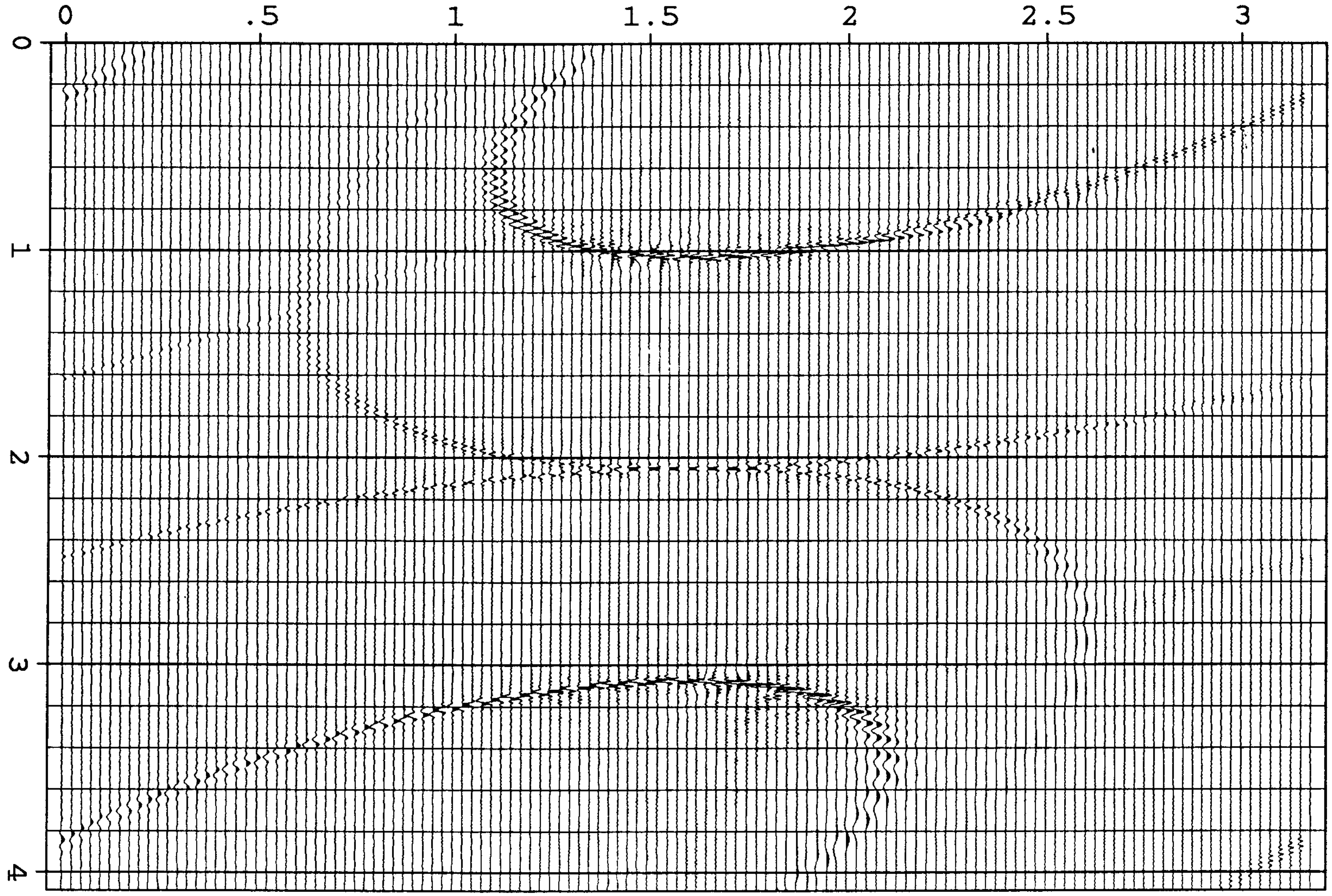
Migration in Helical Coordinates